

Neuron-centric Hebbian Learning

Andrea Ferigo
andrea.ferigo@unitn.it
University of Trento
Trento, Italy

Elia Cunegatti
elia.cunegatti@unitn.it
University of Trento
Trento, Italy

Giovanni Iacca
giovanni.iacca@unitn.it
University of Trento
Trento, Italy

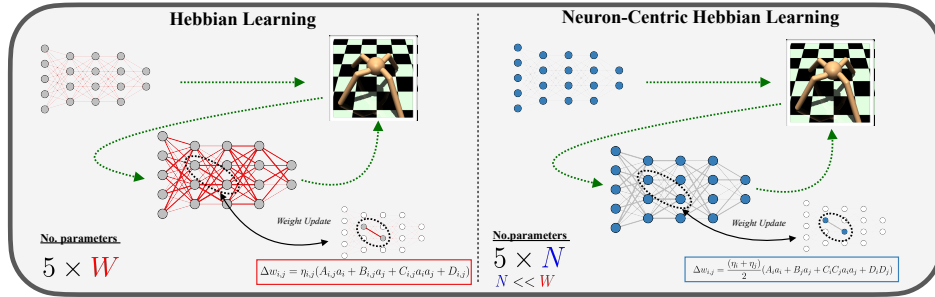


Figure 1: Graphical representation of the traditional **HL** (left) and our Neuron-centric Hebbian Learning model (right). Regarding **HL**, when the network is initialized (first arrow) it starts a loop of observations and actions, in which **HL** updates the weights (black arrow) by using the equation shown in the red box (see also Equation (2)). As can be seen, the parameters of the Hebbian rule in **HL** are specific to each synapse, leading to a total of $5W$ parameters to optimize, with W being the number of synapses. Alternatively, our **NcHL** model (right) updates the weights (black arrow) by using the equation shown in the blue box (see also Equation (3)). In this case, the parameters of the Hebbian rule are specific to each neuron, hence resulting in a total of $5N$ parameters to optimize, with N being the number of neurons. Assuming $N \ll W$, optimizing **NcHL** models becomes notably less difficult than optimizing **HL** models, yet achieving comparable performance.

ABSTRACT

One of the most striking capabilities behind the learning mechanisms of the brain is the adaptation, through structural and functional plasticity, of its synapses. While synapses have the fundamental role of transmitting information across the brain, several studies show that it is the neuron activations that produce changes on synapses. Yet, most plasticity models devised for artificial Neural Networks (NNs), e.g., the ABCD rule, focus on synapses, rather than neurons, therefore optimizing synaptic-specific Hebbian parameters. This approach, however, increases the complexity of the optimization process since each synapse is associated to multiple Hebbian parameters. To overcome this limitation, we propose a novel plasticity model, called Neuron-centric Hebbian Learning (NcHL), where optimization focuses on neuron- rather than synaptic-specific Hebbian parameters. Compared to the ABCD rule, NcHL reduces the parameters from $5W$ to $5N$, being W and N the number of weights and neurons, and usually $N \ll W$. We also devise a “weightless” NcHL model, which requires less memory by approximating the weights based on a record of neuron activations. Our experiments on two robotic locomotion tasks reveal that NcHL performs comparably to the ABCD rule, despite using up to ~ 97 times less parameters, thus allowing for scalable plasticity.

Permission to make digital or hard copies of part or all of this work for personal or classroom use is granted without fee provided that copies are not made or distributed for profit or commercial advantage and that copies bear this notice and the full citation on the first page. Copyrights for third-party components of this work must be honored. For all other uses, contact the owner/author(s).
GECCO '24, July 14–18, 2024, Melbourne, VIC, Australia
© 2024 Copyright held by the owner/author(s).
ACM ISBN 979-8-4007-0494-9/24/07.
<https://doi.org/10.1145/3638529.3654011>

CCS CONCEPTS

• **Computing methodologies** → **Neural networks**; *Genetic algorithms*; *Artificial life*; • **Theory of computation** → **Models of learning**.

KEYWORDS

Neural networks, plasticity, pruning, neuroevolution

ACM Reference Format:

Andrea Ferigo, Elia Cunegatti, and Giovanni Iacca. 2024. Neuron-centric Hebbian Learning. In *Genetic and Evolutionary Computation Conference (GECCO '24)*, July 14–18, 2024, Melbourne, VIC, Australia. ACM, New York, NY, USA, 9 pages. <https://doi.org/10.1145/3638529.3654011>

1 INTRODUCTION

In the natural world, the number of neurons in the brain can vary by several orders of magnitude, from 302 in the nematode worm [46] to 70 billion in Humans [14]. As known, these cells do not act independently, but it is their interaction that creates the complex network that we refer to as the brain. This complex system shows the capability to solve complex, heterogeneous tasks and adapt to new and unforeseen situations. This kind of adaptation is currently still limited in modern Artificial Intelligence (AI) systems.

One of the most important mechanisms that directly affects the adaption capability of the brain is the *synaptogenesis*, which regulates the growth and pruning of the synapses over the life span of an organism. For example, during the lifetime of a person, there is a growing phase where the number of synapses reaches a staggering number of 4 quadrillion synapses, eventually decreasing during adulthood and stabilizing at around 500 trillion [6, 50].

Recent attempts tried to replicate this process in artificial Neural Networks (NNs) [9], or characterize the similarity between natural and artificial NNs [48].

The second important mechanism behind brain adaptation is its way to *change the strength* of its synapses, based on the frequency with which they are used. This process, originally described by Hebb in [13], is at the base of the concept of *plasticity*. Differently from the well-known (but, somehow less biologically plausible) gradient-based backpropagation, which is a supervised learning mechanism based on backward propagation (from outputs to inputs) of errors over a NN, Hebbian Learning (**HL**¹) is a biologically plausible mechanism that allows learning by only propagating information *forward* (from inputs to outputs) over the network.

Different **HL** models have been proposed in the literature, addressing various tasks such as computer vision classification [19], test-time adaptation [43], and Reinforcement Learning (RL) for robotics [8, 20], where, e.g., a robot needs to learn how to perform locomotion [10] or maze navigation [47], or adapt to unforeseen situations, such as damages in its morphology [31]. However, the existing **HL** methods focus on the synapses, i.e., each connection has its own Hebbian rule to control the weight update, with its corresponding parameters. Hence, from an optimization perspective, the number of parameters to optimize in a Hebbian model increases linearly with the number of synapses in the network. This makes the training of **HL** models more computationally demanding.

In this work, we address this issue from a biologically plausible perspective. Leveraging on the intuition that, in **HL**, it is the activation of the neurons that produces a change of the synapses, we depart from the traditional, *Synaptic-centered* **HL** paradigm to propose a novel, *Neuron-centric Hebbian Learning* model (in short, **NcHL**) where the parameters of the Hebbian update rule are specific to neurons rather than synapses. This leads to a significant decrease in the number of parameters of the models, as the number of neurons in an NN can be orders of magnitude smaller than the number of synapses. Moreover, even though in our model the parameters of the update rule are specific to each neuron rather than each synapse, the model still allows for specialization of the synaptic updates, thanks to the effect of the parameters associated to the pre- and post-synaptic neurons connected to each synapse.

As a second contribution of this work, we then reduce the **NcHL** model to what we call a “weightless” version of it (**WNcHL**). This model does not use the weights to calculate the activations, but each neuron stores a record of previous activations and uses these values to calculate the weights without explicitly storing them.

We tested our method on two simulated robotic locomotion tasks, one involving Voxel-based Soft Robots (VSR) [26], and one involving a quadruped robotic task from the MuJoCo suite [44], simulated in the PyBullet physics engine [4]. For these robots, we used Feed-Forward NNs of different sizes, moving from the smallest network with only 13 neurons and 30 synapses, to the biggest one with 420 neurons and 40960 synapses.

In a first set of experiments, our results showed that the **NcHL** model reaches comparable performance as the traditional **HL** model for all the tasks and NNs tested. However, the **NcHL** model needs

to optimize up to ~ 97 times less parameters. In a second set of experiments, we then tested the **WNcHL** model and observed that optimizing its Hebbian parameters requires $\sim 99.7\%$ less memory than **NcHL**, while losing only between $\sim 17\%$ and $\sim 37\%$ of the performance. Finally, we compared the behavior of the **HL** and **NcHL** models, showing that the two models tend to explore the behavioral space following similar trajectories.

The rest of this paper is organized as follows. Section 2 introduces the background and summarizes the related works. Section 3 describes the methods. Section 4 presents the experimental setup and the numerical results, followed by the conclusions in Section 5.

2 BACKGROUND AND RELATED WORK

Plasticity refers to the capability of the brain to adapt internally, in order to learn to deal with new situations during the agent’s lifetime, a fundamental property for both natural [1] and artificial learning systems [15, 23].

In living organisms, plasticity derives from the capability of the brain to create, change, or destroy, its synapses. Creating and destroying synapses are seen as a form of *structural plasticity* [39], as they lead to a direct modification of the structure of the brain [36, 49]. Changing (i.e., strengthening or weakening) the existing synapses, instead, is seen as a form of *functional plasticity*, as it modifies the processing function of the brain. More specifically, the capability of the brain to change the strength of synapses, based on the activations of the neurons they connect, is known as Hebbian Learning (**HL**) [3, 13], which postulates that neurons that often fire together will eventually strengthen their connection, while neurons that do not influence each other will tend to weaken it.

Structural plasticity. The concepts above have been extensively studied in artificial NNs. In particular, structural plasticity has been translated into various approaches to *pruning* and *network development*. The former consists of selecting some synapses to be removed from a dense (i.e., fully connected) NN, without affecting its performance. In this case, the overall size of the network (in terms of number of neurons) does not change, while the number of parameters (i.e., weights) can be greatly decreased [12, 16, 29]. The recent literature has thoroughly studied the most relevant characteristics of sparse NNs, both for Feed-Forward [24, 42] and Convolutional NNs [5, 34]. Another work [48] observed structural similarity between high-performing sparse NNs and biological systems [2].

Network development, instead, takes a different approach. It builds the NN from an initial (typically small, random) structure, to evolve it into a more complex, possibly more efficient one [9, 32]. In this case, both neurons and synapses are iteratively added to the network, to improve its capacity to learn on the given task.

Functional plasticity (Hebbian Learning). Functional plasticity in artificial NNs refers to the capability of the network to change its weights during the execution of a certain task. In this case, **HL** specifically refers to how weights are updated based on a given *Hebbian rule*, which determines the perturbation to be applied to the weights at each step of the task execution. These rules can be either discovered through an optimization process, such as Genetic Programming [18] or autoML [38] (as done in [22]) or, most frequently, handcrafted before the task execution. In this latter case,

¹In this paper, we will use **HL** to refer to the traditional, Synaptic-Centric Hebbian Learning model (including the ABCD rule model), to distinguish it from our proposed Neuron-centric Hebbian Learning model, referred to as **NcHL**.

the Hebbian rules are based on a fixed parametric formulation, and only the parameters of such rules are optimized.

It is worth noticing that, differently from gradient-based back-propagation, Hebbian learning does not require any backward pass. In fact, the NNs weights are updated following the selected Hebbian rules after at *each forward step*. To better evaluate the Hebbian parameters, the performance of an agent is computed *globally* w.r.t. the cumulative reward over the task, rather than *locally*, i.e., as the performance at each forward step. During this process, the Hebbian rule is fixed, and its parameters are typically updated through evolutionary optimization.

Different Hebbian rules can be found in the literature [41]. One of the most established models is the so-called *ABCD rule*, which has been proven effective in different tasks, achieving comparable or better performance w.r.t. non-plastic NNs [10, 25, 31, 33]. In this model, each weight $w_{i,j}$ is updated as:

$$w_{i,j} = w_{i,j} + \Delta w_{i,j} \quad (1)$$

where $\Delta w_{i,j}$ is a function $h(a_i, a_j)$ calculated as follows:

$$\Delta w_{i,j} = \eta_{i,j} (A_{i,j}a_i + B_{i,j}a_j + C_{i,j}a_i a_j + D_{i,j}) \quad (2)$$

where $\eta_{i,j}$ is the learning rate, $A_{i,j}$ modulates the activation of the pre-synaptic neuron (a_i), $B_{i,j}$ modulates the activation of the post-synaptic neuron (a_j), $C_{i,j}$ modulates the mutual interaction of the two activations (a_i, a_j) and $D_{i,j}$ is a bias. Namely, the A , B , C , and D parameters can be seen as the weights of a non-linear combination (scaled by the learning rate η) of the pre and post-synaptic activation values and a unitary bias. If one of the four parameters is greater than the others (in absolute value), it means that the corresponding input value is more relevant to the output (i.e., $\Delta w_{i,j}$) than the other inputs. For instance, if the bias (associated with D) turns out to be the only relevant (i.e., non-null) input value, $\Delta w_{i,j}$ will not be affected by the activation values but rather will have a fixed increase. We suppose that this could happen in cases where the previous forward steps do not influence the next one (i.e., in a classification task where subsequent samples are uncorrelated, hence the forward step does not depend on the previous ones).

In principle, it could be possible that one single set of parameters (A, B, C, D , plus, possibly, η) is for all the synapses in the network (i.e., $A_{i,j} = A; B_{i,j} = B; C_{i,j} = C; D_{i,j} = D; \eta_{i,j} = \eta \forall i, j$). However, this approach would not allow for specialization of the weight updates across the different parts of the network, hence resulting in ineffective learning [10, 31]. Hence, the majority of works dealing with the ABCD rule in practice optimize a set of 5 parameters for *each synapse*. The drawback of this approach is, obviously, that the total number of parameters to optimize increases from W (i.e., the number of weights) as in traditional NN training, to $5W$, since each synapse is associated to a set of 5 different parameters. This is a common aspect across various plasticity models in the literature [10, 31, 40], with some exceptions such as [47] where, in order to reduce the number of HL parameters, $\Delta w_{i,j}$ is set to $\eta_{i,j} m_{i,j} a_i a_j$, where $\eta_{i,j}$ is a learning rate and $m_{i,j}$ is a neuro-modulatory signal, with both $\eta_{i,j}$ and $m_{i,j}$ being optimized separately for each synapse. Another method from the literature to reduce the number of parameters is the merging procedure described in [37]: during the evolution, this algorithm merges similar rules using k-means and then starts a new optimization with the merged model. Repeating this procedure, the

number of parameters is halved until a desired value. However, this operation requires restarting the evolutionary process increasing the number of iterations, and requires a clustering method.

Novelty of the proposed approach. In this work, we shift the focus of the Hebbian update rules from synapses to the neurons, to better mimic the behavior of biological brains [3], where neurons, rather than synapses, are the elements of specialization. This paradigm shift allows us to greatly reduce the number of parameters to optimize, as the number of neurons (N) in an NN is, apart from the case of heavily sparsified networks, several times lower than the number of synapses (W). As we will see in the next section, this is the main advantage of our proposal.

3 METHODS

As seen in the previous section, given an NN with W synapses, the traditional ABCD rule optimizes $5W$ parameters. Here, we first present our **NcHL** model that reduces the number of parameters to optimize to just $5N$, where N is the number of neurons, rather than synapses in the NN (as said, we can assume that $N \ll W$). Then, we discuss the formalization of **NcHL**, as well as its “weightless” variant (**WNcHL**), which is based on an approximation based on the previous neuron activations and is specifically designed to avoid storing weight parameters at all. Finally, we present the Evolution Strategies algorithms that we use to optimize our models².

3.1 Neuron-centric Hebbian Learning

The main idea behind our proposed **NcHL** model is to specialize the weight update at the level of neuron rather than synapse, still preserving the inherent independence of the traditional ABCD rule w.r.t. the reward of the given task. In other words, the weight update is solely regulated by the activations of the pre- and post-synaptic neurons i and j . However, differently from the traditional ABCD rule, see Equation (2), where the parameters $A_{i,j}$, $B_{i,j}$, $C_{i,j}$, $D_{i,j}$, and $\eta_{i,j}$ can be specific to each synapse, in **NcHL** the Hebbian rule parameters are specific to *each neuron*, i.e., each neuron has a different set of 5 parameters, and each weight $w_{i,j}$ is updated according to the following update rule: $h(a_i, a_j)$:

$$\Delta w_{i,j} = \frac{(\eta_i + \eta_j)}{2} (A_i a_i + B_j a_j + C_i C_j a_i a_j + D_i D_j) \quad (3)$$

where: the learning rate is calculated as $\frac{(\eta_i + \eta_j)}{2}$, i.e., we consider the average learning rate of the pre- and post-synaptic neurons; A_i and B_j are associated, respectively, to the pre-synaptic neuron i and the post-synaptic neuron j , and modulate their corresponding activations; the product $C_i C_j$ modulates the co-contribution of the activations of the pre- and post-synaptic neurons; the product $D_i D_j$ is calculated by multiplying the bias associated to the pre- and post-synaptic neurons.

Even though the Hebbian rule update shown in Equation (3) turns out to be more complex compared to the traditional ABCD rule, it is important to note that the total number of parameters in the whole network greatly decreases, as we will demonstrate in Section 4. In the traditional model, the total number of parameters to optimize increases linearly with the number of synapses. Instead,

²Our codebase is publicly available at <https://github.com/ndr09/NCHL>.

in **NcHL** it increases linearly with the number of neurons, hence resulting in a smaller number of parameters to optimize.

3.2 Neuron-centric Hebbian Learning “weightless”

With the **NcHL** model, we reduce the number of parameters needed to *store* from $6W$ for the traditional ABCD model (W weights plus $5W$ Hebbian rule parameters) to $W + 5N$ (W weights plus $5N$ Hebbian rule parameters). Here, we further propose a new Hebbian model aiming to further reduce the memory needed to store the model parameters. In particular, rather than storing the weights in memory, we approximate them using the **NcHL** update rule. Hence, we call this this model “weightless” **NcHL** (in short, **WNcHL**).

To explain the rationale behind this model, we start with the following considerations. Let us assume we have two neurons i (pre-synaptic) and j (post-synaptic) with their respective activations a_i and a_j , which are linked by $w_{i,j}$. Now, if we assume that the initial value of $w_{i,j}$, $w_{i,j}^0$, is 0^3 , we can express the value of the activation of the post-synaptic neuron j at step T as $a_j^T = f(w_{i,j}^T a_i^T)$, where $f(\cdot)$ is the activation function and $w_{i,j}^T = \sum_{t=0}^T h(a_i^t, a_j^t)$, where $h(\cdot)$ is the Hebbian update rule expressed in Equation (3)⁴. In other words, by computing $h(a_i^t, a_j^t) = \Delta_{i,j}$ for each step t , we can find the value of $w_{i,j}$ at step T . This means that, rather than storing $w_{i,j}$, it is possible to calculate it only based on the history of pre-synaptic and post-synaptic activations over the various steps until T .

However, storing the activations for all steps will lead to using more memory than what is needed if we store the weights. Hence, rather than considering the whole history of steps until T , we store only a subset of the last activations, aiming to reduce memory consumption. We call this subset the *memory window*, whose size is M_w . Therefore, we approximate the weight values as follows:

$$w_{i,j}^{M_w} = \sum_{t=0}^{M_w} h(a_i^t, a_j^t). \quad (4)$$

In other words, to calculate $w_{i,j}^{M_w}$, it is enough to store the activations of the neurons over M_w steps in the memory window.

3.3 Evolution Strategies

To optimize the Hebbian rules, we employ two Evolution Strategies (ES). The first one, provided in [28], creates a new population of m solutions in two steps: firstly, it selects the n best solutions and calculates the vector \mathbf{g}_{mean} as the mean of these solutions, namely $\mathbf{g}_{mean} = 1/m \sum_{i=0}^m \mathbf{g}_i$. Then, it generates $m - 1$ new solutions by adding to each variable of \mathbf{g}_{mean} a random value sampled from $\mathcal{N}(0, \sigma)$. Finally, the algorithm composes the new population by combining the $m - 1$ new solutions with the best solution from the previous generation. We refer to this algorithm as ES₁.

The second algorithm, from [31], generates the new population by updating the solutions based on their fitness. For each solution \mathbf{g} in a population of size m , a random perturbation $\mathcal{N}(0, \sigma)$ is added to each variable, $\mathbf{g}' = \mathbf{g} + \mathcal{N}(0, \sigma)$. Then, based on the fitness of the

³Since reducing the memory needed to store the model parameters is the main requirement of the proposed **WNcHL** method, this assumption allows us to avoid storing W additional parameters for the initial values of the weights.

⁴Note that, in principle, this can be applied also to the traditional ABCD rule in Equation (2). However, in this case, the reduction in terms of the number of parameters would be only W .

solution, each parameter of \mathbf{g}' is updated as follows: $\mathbf{g}'' = lr/(m\sigma) + \sum_{i=0}^m \mathbf{g}_i' F(\mathbf{g}_i')$. Note that σ and lr decay over the generation by a factor lr_{decay} and σ_{decay} . We refer to this algorithm as ES₂.

4 EXPERIMENTS

We performed a suite of experiments aimed at answering the following research questions:

- RQ1 How does **NcHL** perform w.r.t. the traditional **HL** model based on the ABCD rule?
- RQ2 Does the **WNcHL** model achieve similar performance w.r.t. **NcHL**?
- RQ3 Since **NcHL** and **HL** models optimize the Hebbian rules parameters respectively w.r.t. neurons and synapses, are the best solutions found by the two models somehow behaviorally similar, or different?

4.1 Experimental setup

Tasks. We tested our model on two simulated locomotion tasks, namely ① one where we employed Voxel-based Soft Robots (VSR) [26, 27], and ② one where we employed the RL task Ant [17] from the MuJoCo suite [44]. The first task has been selected for being somehow easier from an optimization perspective. Hence, we tested it on smaller NNs. On the other hand, the second task, which is well-established for its complexity, has been selected to test the scalability of our approach, as this task requires much larger NNs in order to be solved effectively. For both tasks, the goal is to make the agent walk the farthest, so the fitness is the distance covered by the robot from the beginning to the end of each task episode.

The first task ① is characterized by robots whose body is composed of voxels (i.e., soft structures that can shrink or expand based on a control signal). Each voxel can sense various information, namely: (1) the velocity of the voxel (along the x and y axes), (2) the ground contact, (3) the area ratio (namely, the compression or expansion of the voxel area w.r.t. its rest surface), and (4) the distance from an obstacle or the terrain (through a Lidar sensor). The locomotion happens in an uneven terrain composed of hills with different slopes, lasting 3600 steps. For this task we relied on the 2D VSR simulator implemented in [26, 27]. We considered two kinds of morphology shapes, namely a 7×1 shape, a.k.a. a *worm*, and a 4×3 shape with a 2×1 “hole” in the central bottom part, a.k.a. a *biped*. We used these shapes as they have been successfully employed in previous works regarding this kind of VSR [10, 11, 30]. We also varied the sensors equipped on these robots, defining three sensory configurations that we refer to respectively as *low*, *medium*, and *high*, depending on the number of sensors present in each voxel. In particular, in the *low* configuration, there are only area ratio sensors, the *medium* configuration uses also the velocity and ground contact sensors, while the *high* configuration uses all four kinds of sensors. The total number of sensor inputs for each configuration is 3, 28, and 31 for the worm and 8, 20, and 29 for the biped, respectively for the *low*, *medium*, and *high* configurations. More details on these three configurations can be found in [10]. In total, we tested six VSR configurations (two shapes, each one with three sensory configurations).

In the second task ②, a 3D quadruped robot, called Ant, has to move as far as possible, for a total of 1000 steps, on a flat terrain

[17]. In this task, the agent has to control 8 actuated joints (two per leg) based on a set of 28 inputs representing the velocity and position of the different parts of the robot. For this task, we used the implementation available in the PyBullet physics engine [4].

Neural network architectures. We used a set of different Feed-Forward NNs for each task. We used the \tanh activation function.

① Regarding the VSR, as discussed before, the number of inputs depends on the sensory configuration and shape of the VSR. As for the number of outputs, it depends on the number of voxels present in the shape, thus 7 for the worm and 10 for the biped. Following [10], all the NNs used for this task have been configured with a single hidden layer with the same size as the input, so in total we have six NN configurations, i.e., one per VSR configuration.

② For the Ant task, the sensory configuration and structure of the robot are fixed. Hence, we tested two different NN configurations with two hidden layers. The first one, which we refer to as *medium* has two layers of sizes 128 and 64, while the second, which we refer to as *high*, has two layers of sizes 256 and 128.

Evolution Strategies. For the eight networks described above (six for VSR and two for Ant), we optimized two Hebbian models, namely the traditional ABCD rule (that we refer to as **HL**), and our proposed **NcHL** model. We report in Table 1 all the parameters (size of input, hidden and output layers) of the NNs used for both tasks, including the different number of parameters to optimize for each network configuration using either **HL** or **NcHL**, along with the ratio of the number of parameters between **HL** and **NcHL**. Note that, in the VSR task the η value is fixed at $\eta = 0.1$ (as in previous works on VSR [10, 11, 30]), while for the Ant task, it is optimized together with the other Hebbian parameters. Also, we should note that, for both ES_1 and ES_2 , we used direct representation, i.e., the algorithms directly evolved the Hebbian parameters of the two models.

For the experiments for RQ1, we decided to use ES_1 for the VSR task, as this algorithm is provided with the VSR simulator [28], while we used ES_2 for the Ant task, as its implementation is already provided with the implementation of the task [31]. For the experiments for RQ2, instead, we preferred to use ES_1 for the Ant task, because of constraints on the computational resources.

ES_1 is, in fact, configured to be less computationally expensive, with a population size of 40, 500 generations, and $\sigma = 0.35$. ES_2 , on the other end, is configured to be more computationally demanding, with a population size of 500, 500 generations, $\sigma = 0.1$, learning rate $lr = 0.2$, $\sigma_{decay} = 0.999$, and $lr_{decay} = 0.995$.

Note that, for the experiments on RQ1 and RQ3, we uniformly initialized the weights of the networks in the range $[-0.1, 0.1]$, while for RQ2 all weights are set to 0. Moreover, we remark that for each experiment and setting in RQ1 and RQ2, we collected the results from 10 independent runs of the corresponding ES.

Random baselines. In both tasks, we also tested two random baselines, which we refer to as **HL**-Random and **NcHL**-Random. **HL**-Random solutions are created by associating, independently for each synapse (i, j) , a Hebbian rule with its parameters $(A_{i,j}, B_{i,j}, C_{i,j}, D_{i,j}, \eta_{i,j})$ uniformly sampled in $[-1, 1]$, see Equation (2). Similarly, **NcHL**-Random solutions are created by associating, independently for each neuron i , a Hebbian rule with its parameters $(A_i, B_i, C_i, D_i, \eta_i)$ uniformly sampled in $[-1, 1]$, see Equation (3).

Since, for the experiments conducted to address RQ1 and RQ2, the performances of these random baselines are close to zero for both tasks, we do not present those results in the analysis of those research questions. Instead, we report the behavior of the random baselines only in the analysis conducted for RQ3.

Table 1: Network description and number of parameters to optimize for the different settings we tested. In the VSR task, we use an NN with a single hidden layer whose size is equal to the input size. Here, the **NcHL model requires optimizing up to ~21 times less parameters than **HL**, depending on the network size. In the Ant task, where we used a 2-hidden layer NN, the advantage of **NcHL** in terms of the number of parameters to optimize w.r.t. **HL** model increases: **NcHL** requires up to ~97 times less parameters than **HL**.**

Task	Shape	NN Configuration	Layer size			No. of parameters		
			Input	Hidden	Output	HL	NcHL	Ratio
VSR	Biped	Low	8	8	10	576	88	6.54
		Medium	20	20	10	2400	160	15.00
		High	29	29	10	4524	214	21.14
	Worm	Low	3	3	7	120	46	2.60
		Medium	28	28	7	3920	196	20.00
		High	31	31	7	4712	214	22.01
Ant	-	Medium	28	128, 64	8	61440	1140	53.89
		High	28	256, 128	8	204800	2100	97.52

4.2 Experimental results

We now present the results of the experiments conducted to answer the three RQs discussed above.

Before going into the details of the three RQs, it is worth highlighting once again that the proposed **NcHL** model significantly reduces the number of parameters to optimize w.r.t. the traditional **HL** model. This trend is clearly visible in Table 1, see in particular the last three columns, where we summarize the number of parameters to optimize in each case. We can observe that the total number of parameters to optimize with the proposed **NcHL** model is one or two orders of magnitude smaller than the **HL** model. In the best case (the “high” configuration on the Ant task) **NcHL** requires ~ 97 times less parameters than **NcHL**.

To further demonstrate this advantage of our model, Figure 2 displays the number of parameters needed (on a toy example of a task with one input and one output) by **HL** and **NcHL** when increasing both the number of hidden layers and neurons therein (note the logarithmic scale on the y-axis). We can clearly observe that **NcHL** requires a substantially smaller number of parameters w.r.t. a **HL** model with the same number of hidden layers.

While this mechanism can reduce the size of the search space, it could also lead to subpar performances as it might be harder for the evolution to find solutions with enough behavioral complexity to solve the task at hand. Therefore, we are interested in studying the performance that our proposed **NcHL** model can achieve w.r.t. the traditional **HL** model. This is the focus of our RQ1.

RQ1: **NcHL vs **HL** performance.** Firstly, we analyzed the results of the VSR task ①. In Figure 3, we report the fitness trends for the different shapes and sensory configurations. We can observe that the **NcHL** and **HL** models show a very similar trend for both the worm and the biped shapes and for all three sensory configurations. In Figure 4, we show the distribution of the distance achieved by the

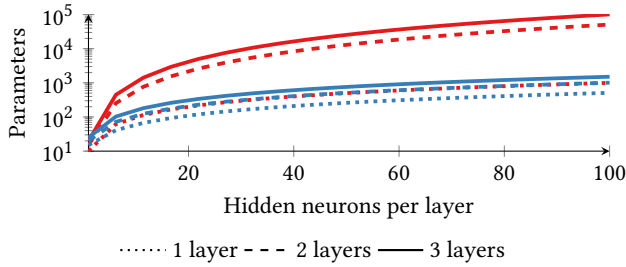


Figure 2: Number of parameters to optimize with HL and NcHL in Feed-Forward NN (toy example, 1 input and 1 output) when varying the no. of hidden layers and neurons therein.

best solution found in each independent run. While, in some cases, the distribution seems slightly different, conducting the TOST test [45] with a bound of 10% on the average fitness returned a p -value greater than 0.05 for all the pairwise comparisons, indicating that the hypothesis of statistical equivalence cannot be rejected.

We then moved to analyze the results from the Ant task ②, to observe if the results obtained with the VSR were due to the lower number of parameters to optimize in that case, or if the NcHL model is also able to scale to bigger NNs. In Figure 5, we show the fitness trend for the two networks we tested on the Ant task. In this case, the trends are slightly different: with the “medium” NN, the NcHL model seems to converge faster, while with the “high” NN, the NcHL model seems to converge slower than the HL model. However, we can observe that eventually, with both networks, the performance of HL and NcHL converge to similar values. We confirmed this in Figure 6, where we plot the average performance over 100 task rollouts (as done in [31]) of the best solutions of each independent run. The NcHL models reach an average score of 1148 ± 98 and 1216 ± 149 for the medium and high configuration (in comparison, a standard RL method such as PPO reaches a score of around 3100 [35]). In this case, the TOST test returned a p -value of 0.26 and 0.66, respectively for the “medium” and “high” models. Hence also in this case we cannot reject the hypothesis of statistical equivalence.

RQ2: WNcHL performance. Aiming to answer the second research question (RQ2), we focused only on the hardest task, i.e., Ant. The only difference w.r.t. to the previous experimental setting is that, in this case, the weights of NcHL are initialized to 0 at the beginning of the task, for a fair comparison with WNcHL where, instead, as seen earlier we assume by construction that there are no initial weights, which allows us to avoid storing them.

For the optimization process, in this set of experiments, we opted for ES₁, with the same parametrization as the previous experiments, preferred over ES₂ due to computational constraints (in fact, it uses a population size that is 12.5 times smaller).

In a first set of experiments, we evolved the NcHL models for 10 independent runs. We then took the best solution found in each run, and, given that the initial weights are set to 0, we applied the WNcHL model, see Equation (4), to each of them. We did that for various sizes of the memory window (M_w) on which the model approximates the weights, to assess its effect on performance. Taking as the biggest possible window the maximum duration of the task (which, in the case of Ant, is 1000 forward steps), we considered progressively increasing values of M_w , from 2 to 1000, with equal

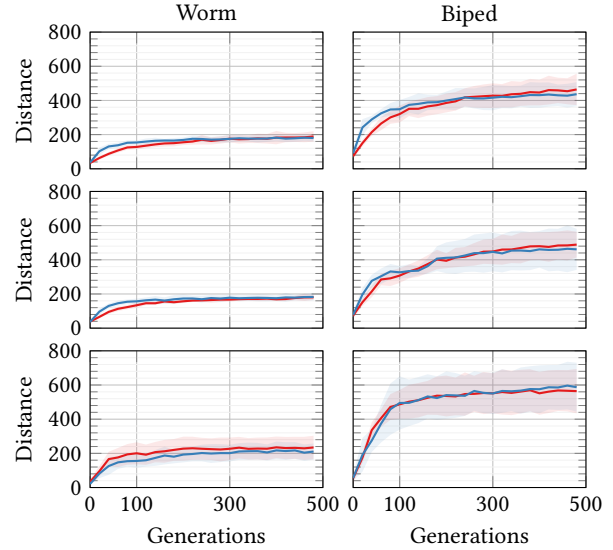


Figure 3: RQ1: Distance trend of the best solution (avg. \pm std. dev. across 10 runs) found at each generation by HL and NcHL in the various configurations of the VSR task. From top to bottom, the results refer to the High, Medium, and Low sensory configurations.

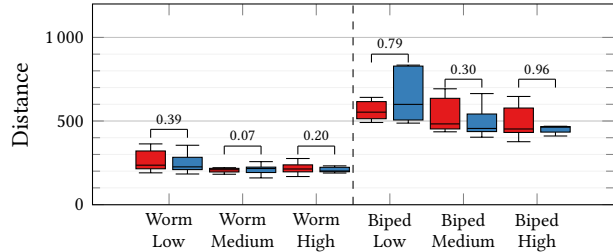


Figure 4: RQ1: Distribution of the best distance achieved across 10 runs by HL and NcHL in the various configurations of the VSR task.

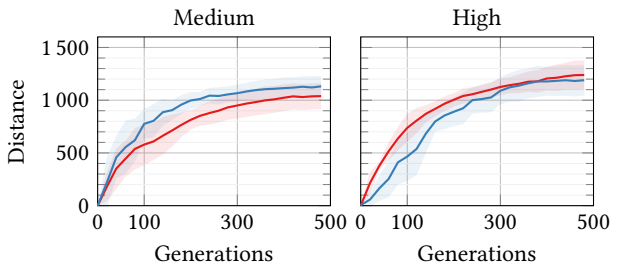


Figure 5: RQ1: Distance trend of the best solution (avg. \pm std. dev. across 10 runs) found at each generation by HL and NcHL in the two configurations of the Ant task.

spacing. We show the average results obtained in Figure 7. In the figure, the orange line shows the ratio between the fitness of the WNcHL model and the fitness of the corresponding NcHL model, namely $F_{ratio} = \frac{F_{WNcHL}}{F_{NcHL}}$, while varying M_w . The black line, instead, shows the ratio between the number of activations stored in WNcHL and the number of weights stored in NcHL.

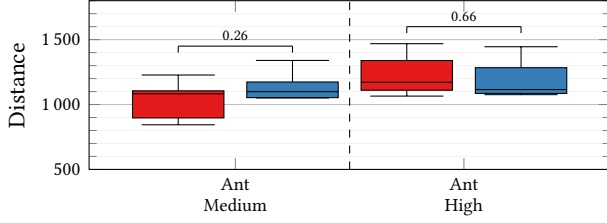


Figure 6: RQ1: Distribution of the average distance in 100 rollouts of each best solution found in each of the 10 runs of HL and NcHL in the two configurations of the Ant task.

We can observe that, as expected, increasing the memory window increases the performance of the WNCnHL model, eventually reaching the same performance as the NcHL model ($F_{ratio} = 1$) when storing all the activations ($M_w = 1000$). However, the memory needed to store the activations values, on which the weights are approximated in WNCnHL, rapidly becomes much bigger than the memory needed to directly store the weights, thus reducing the memory advantage of the WNCnHL approach over the NcHL model.

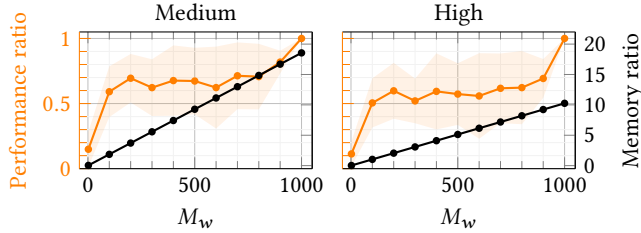


Figure 7: RQ2: Ratio of the performance of the NcHL model w.r.t. the WNCnHL model (orange line) with different memory windows M_w (avg. \pm std. dev. across the best solution found in each of 10 runs of NcHL, and then converted it to the corresponding WNCnHL model, on the Ant task). We also indicate the ratio between the memory consumption in terms of the number of activations (for WNCnHL) and the number of weights (for NcHL) in two models (black line).

Therefore, given the relevant drop in memory efficiency for large values of the memory window, we performed a second experiment, where we set $M_w = 2$, and optimized the Hebbian parameters for this WNCnHL model. We show these results in Figure 8. While the performance of the WNCnHL model does not reach the same performance of the NcHL model (we verified this with the Mann-Whitney U test, which returned a p -value equal to 0.009 and 0.008, respectively for the “medium” and “high” configuration), we can see how the WNCnHL model still reaches fairly good performances, especially in the “medium” case. Moreover, optimizing the Hebbian parameters leads to an increase in the F_{ratio} from 0.14 and 0.11 to 0.83 and 0.64, respectively for the “medium” and “high” models.

Summarizing, we observed that, using, for the “medium” network, only $M_{ratio} = \frac{M_w \times N}{W} = \frac{2 \times 228}{12880} \approx 0.03\%$ of the memory of NcHL, we lost only $\sim 17\%$ of performance (see the final distance achieved by the two models shown in Figure 8). Correspondingly, for the “high” network the memory consumption of WNCnHL is $\sim 0.02\%$ of NcHL with a performance drop of $\sim 37\%$. While this performance drop can be considered significant, there might be cases where this performance-memory trade-off could be acceptable. For

instance, the “high” network with the NcHL model needs to store 40960 weights, 2100 Hebbian rule parameters, and 392 activations, for a total of 43452 values. Considering 32-bit float-point representation, this model would need ~ 170 KB (as a concrete example, an Arduino Nano has only 30KB of Flash Memory available). In comparison, the WNCnHL model with $M_w = 2$ requires storing 2 activations and the 5 Hebbian rule parameters for each neuron (for a total 420 neurons), hence requiring ~ 11 KB of memory. Therefore, NcHL requires about 15 times more memory than WNCnHL.

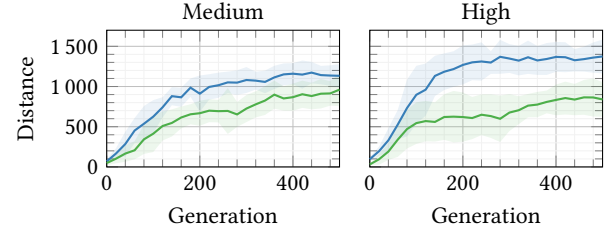


Figure 8: RQ2: Distance trend of the best solution (avg. \pm std. dev. across 10 runs) found at each generation by NcHL and WNCnHL in the two configurations of the Ant task.

RQ3: Behavior analysis. To conclude our experiments, we performed a qualitative behavioral analysis of the final networks obtained with both HL and NcHL. As shown in our RQ1 experiments, the final fitness results, as well as their overall trend, for the networks trained with these two different approaches turn out to be very close. Hence, we further investigated the reason behind such a trend. For this analysis, we considered only the most difficult task, i.e., Ant, because the bigger-sized networks used to solve it (see the “medium” and “high” NNs in Table 1) should be able to provide more information on the models’ behavior.

The first step was to analyze the similarity among the activations of HL and NcHL. However, we discovered that, after just a few steps, all the activations in both models go to the maximum/minimum values of \tanh (i.e., -1 or 1). We hypothesized that such behavior on the activations is due to the lack of normalization of the network weights (which was done following the setting of the original study from which the Ant task is taken [31]). Of note, this pattern can however be linked to several biological studies [7, 21] that discuss the “all-or-nothing” behavior of biological neurons, i.e., the fact that such neurons do not have an intermediate activation value: they either fire, or not.

Hence, we decided to better analyze the network similarity by relying on the behavioral trajectories. For each of the best solutions found in each of 10 evolutionary runs on HL and NcHL for RQ1, we extracted the trajectories from 3 test rollouts. Likewise, we created 10 individuals for both HL-Random and NcHL-Random, and tested them over 3 rollouts. For each trajectory, we stored three pieces of information for every forward step (the total number of steps being 1000), namely the input values $I \in \mathbb{R}^{1 \times 28}$, the pre-synaptic $P \in \mathbb{R}^{1 \times 8}$, and the post-synaptic activations of the last layer $P' \in \mathbb{R}^{1 \times 8}$. Note that with pre-synaptic activations, we mean the values of the output layer before the activation function, hence the values are in the range $[-\infty, \infty]$. While with post-synaptic activations, we mean the values after the activation function, hence they are in the range $[-1, 1]$.

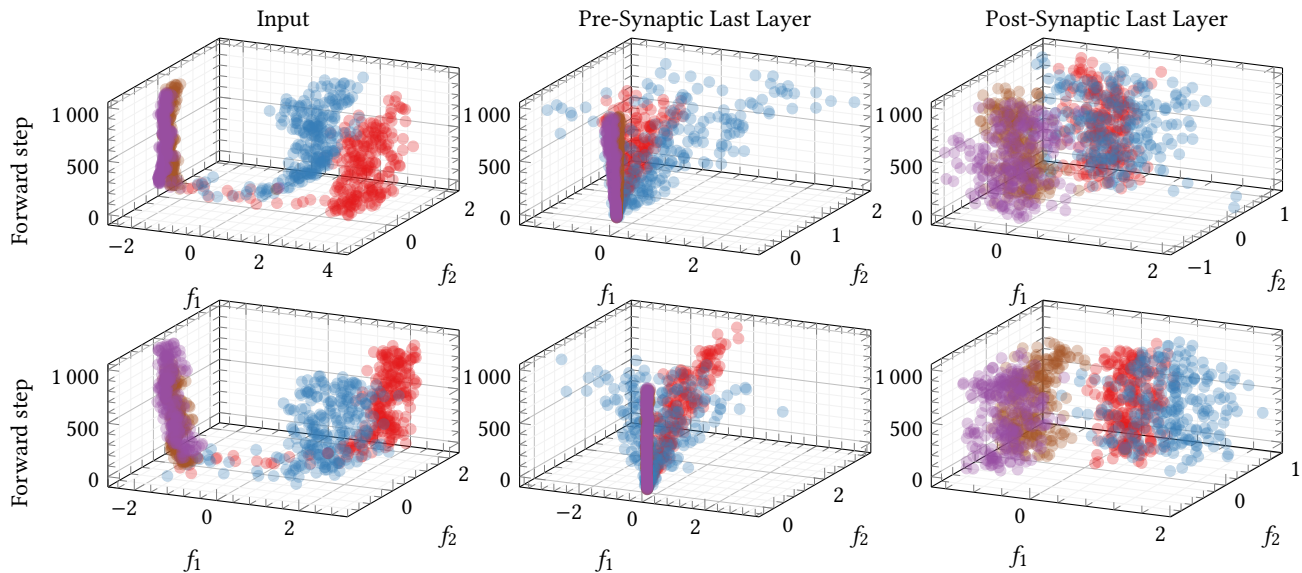


Figure 9: RQ3: Average trajectory at various network layers (Input layer; Pre-Synaptic Last Layer; Post-Synaptic Last Layer) of the best solutions found on the Ant task (top row: Medium; bottom row: High) from 3 rollouts of each of the best solutions found in 10 evolutionary runs of HL, NcHL, HL-Random, and NcHL-Random, each one tested in 3 rollouts. Each point is a 2D projection (through PCA) of an n-dimensional vector corresponding to each of the shown layers at a certain forward step.

We conducted this analysis performing, for each of the 30 trajectories of each model, a PCA for each step, separately over the input, pre-synaptic, and post-synaptic values. Then, we calculated for each step the average over all the PCA results of the 30 trajectories.

The averaged trajectories of each algorithm, shown in Figure 9 indicate that: (1) HL and NcHL explore the behavioral space more than the random baselines; (2) the HL and NcHL trajectories turn out to overlap, being separate from the random cases. Analyzing such results from left (input) to right (post-synaptic) over Figure 9 (top row: “medium” network; bottom row: “high” network), it is clear how the input trajectories of HL and NcHL are similar in the “medium” networks, while they almost completely overlap in the “high” case. On the contrary, the random baselines overlap in both cases and remain close to the starting 2D point (the z-axis corresponds to the forward steps). A similar trend is visible in the second column, where the random baselines move along a straight line over the forward axis, while HL and NcHL follow a more complex, but similar trajectory. In the last column, the post-synaptic values (which, as discussed before, turn out to be either -1 or 1), confirm that HL and NcHL explore the behavioral space similarly, and more than the random baselines.

These findings allow us to empirically show one of the reasons behind the similar performance obtained by HL and NcHL over the experiments reported in RQ1. Although our proposed NcHL significantly reduces the number of parameters to be optimized, its ability to explore the behavior space turns out to be as effective as that of the traditional, but more parametrized ABCD rule.

5 CONCLUSIONS

In this paper, we have introduced a novel variant of HL that focuses on neurons rather than synapses. We called this model Neuron-centric Hebbian Learning (NcHL), to highlight the fact that the Hebbian update rule is focused, by design, on neurons. We then

proposed a further “weightless” model (WNcHL), that allows for plasticity but without the need for storing weights. We tested the proposed models on two simulated robotic locomotion tasks in various configurations, showing their effectiveness both in terms of performance and number of parameters. Our experiments showed that, despite a massive reduction in the overall number of parameters to optimize w.r.t. the traditional HL model, NcHL provides comparable performance on the two tasks at hand. On the other hand, WNcHL resulted slightly less competitive than NcHL, which reveals its trade-off between performance and memory-saving.

We concluded our study with a behavioral characterization of HL and NcHL, in comparison with two random baselines. This analysis provided some interesting insights as to what concerns the way NcHL explores the behavioral space following somehow similar trajectories w.r.t. HL, but differently from the random baselines.

In our opinion, this work could represent a first step towards a radical rethinking of HL, since as said we put the emphasis of the Hebbian update on the neurons rather than synapses. To the best of our knowledge, no prior work proposed such a way of formulating HL. Furthermore, our work allows us to preserve a biologically plausible model while reducing the number of parameters, thus paving the way to scalable HL models. Of note, in this work we did not compare our method with alternative approaches to model size reduction, or more advanced HL models: given that our goal was to find a novel way to achieve scalability (from the optimization viewpoint) in HL, rather than improve the performance of HL, we thought that the most meaningful baseline was the vanilla Synaptic-centric HL. Therefore, further investigations are needed to assess the performance of NcHL, also in comparison with alternative learning approaches, and its generalizability e.g. to deep learning scenarios and complex high-dimensional tasks such as computer vision.

REFERENCES

- [1] James Mark Baldwin. 2018. A new factor in evolution. *American Naturalist* 30, 355 (2018), 536–553.
- [2] Danielle Smith Basset and ED Bullmore. 2006. Small-world brain networks. *The neuroscientist* 12, 6 (2006), 512–523.
- [3] Thomas H Brown, Edward W Kairiss, and Claude L Keenan. 1990. Hebbian synapses: biophysical mechanisms and algorithms. *Annual review of neuroscience* 13, 1 (1990), 475–511.
- [4] Erwin Coumans and Yunfei Bai. 2016–2021. PyBullet, a Python module for physics simulation for games, robotics and machine learning. <http://pybullet.org>.
- [5] Elia Cunegatti, Doina Bucur, and Giovanni Iacca. 2023. Peeking inside Sparse Neural Networks using Multi-Partite Graph Representations. [arXiv:2305.16886](https://arxiv.org/abs/2305.16886).
- [6] David A. Drachman. 2005. Do we have brain to spare? *Neurology* 64, 12 (2005), 2004–2005.
- [7] Roger Eckert, R Randall, George Augustine, et al. 1988. *Animal physiology: mechanisms and adaptations*. WH Freeman & Co., New York, NY, USA.
- [8] Karim El-Laithy and Martin Bogdan. 2011. A reinforcement learning framework for spiking networks with dynamic synapses. *Computational Intelligence and Neuroscience* 2011 (2011), 4–4.
- [9] Andrea Ferigo and Giovanni Iacca. 2023. Self-Building Neural Networks. In *Conference on Genetic and Evolutionary Computation Companion*. ACM, New York, NY, USA, 643–646.
- [10] Andrea Ferigo, Giovanni Iacca, Eric Medvet, and Federico Pigozzi. 2022. Evolving Hebbian learning rules in voxel-based soft robots. *IEEE Transactions on Cognitive and Developmental Systems* (early access) (2022), 11.
- [11] Andrea Ferigo, LB Soros, Eric Medvet, and Giovanni Iacca. 2022. On the Entanglement between Evolvability and Fitness: an Experimental Study on Voxel-based Soft Robots. In *ALIFE 2022: The 2022 Conference on Artificial Life*. MIT Press, Cambridge, MA, USA, 10 pages.
- [12] Trevor Gale, Erich Elsen, and Sara Hooker. 2019. The state of sparsity in deep neural networks. [arXiv:1902.09574](https://arxiv.org/abs/1902.09574).
- [13] Donald Olding Hebb. 2005. *The organization of behavior: A neuropsychological theory*. Psychology Press, London, UK.
- [14] Suzanaerculano-Houzel. 2009. The human brain in numbers: a linearly scaled-up primate brain. *Frontiers in human neuroscience* 3 (2009), 31.
- [15] Geoffrey E Hinton, Steven J Nowlan, et al. 1996. How learning can guide evolution. *Adaptive individuals in evolving populations: models and algorithms* 26 (1996), 447–454.
- [16] Torsten Hoefler, Dan Alistarh, Tal Ben-Nun, Nikoli Dryden, and Alexandra Peste. 2021. Sparsity in Deep Learning: Pruning and growth for efficient inference and training in neural networks. *Journal of Machine Learning Research* 22, 241 (2021), 1–124.
- [17] John Schulman and Philipp Moritz and Sergey Levine and Michael Jordan and Pieter Abbeel. 2018. High-Dimensional Continuous Control Using Generalized Advantage Estimation. [arXiv:1506.02438](https://arxiv.org/abs/1506.02438).
- [18] Jakob Jordan, Maximilian Schmidt, Walter Senn, and Mihai A Petrovici. 2021. Evolving interpretable plasticity for spiking networks. *Elife* 10 (2021), e66273.
- [19] Adrien Journé, Hector Garcia Rodriguez, Qinghai Guo, and Timoleon Moraitis. 2023. Hebbian Deep Learning Without Feedback. In *International Conference on Learning Representations*. ICLR, Appleton, WI, USA, 14 pages.
- [20] Jacques Kaiser, Michael Hoff, Andreas Konle, J. Camilo Vasquez Tieck, David Kappel, Daniel Reichard, Anand Subramoney, Robert Legenstein, Arne Roennau, Wolfgang Maass, and Rüdiger Dillmann. 2019. Embodied Synaptic Plasticity With Online Reinforcement Learning. *Frontiers in Neurorobotics* 13 (2019), 11 pages.
- [21] James W Kalat. 2016. *Biological psychology*. Cengage Learning, Singapore.
- [22] Stephen Kelly, Daniel S. Park, Xingyou Song, Mitchell McIntire, Pranav Nashikkar, Ritam Guha, Wolfgang Banzhaf, Kalyanmoy Deb, Vishnu Naresh Boddeti, Jie Tan, and Esteban Real. 2023. Discovering Adaptable Symbolic Algorithms from Scratch. In *IEEE/RSJ International Conference on Intelligent Robots and Systems*. IEEE, New York, NY, USA, 3889–3896.
- [23] Wei Li, Edgar Buchanan Berumen, Léni Le Goff, Emma Hart, Matthew Hale, Matteo De Carlo, Robert Woolley, Alan Winfield, Jon Timmis, AE Eiben, et al. 2023. Evaluation of frameworks that combine evolution and learning to design robots in complex morphological spaces. *IEEE Transactions on Evolutionary Computation* (Early Access) (2023), 15 pages.
- [24] Shiwei Liu, Tim Van der Lee, Anil Yaman, Zahra Atashgahi, Davide Ferraro, Ghada Sokar, Mykola Pechenizkiy, and Decebal Constantin Mocanu. 2021. Topological insights into sparse neural networks. In *Joint European Conference on Machine Learning and Knowledge discovery in databases*. Springer, Cham, Switzerland, 279–294.
- [25] Claudio Mattiussi and Dario Floreano. 2007. Analog genetic encoding for the evolution of circuits and networks. *IEEE Transactions on evolutionary computation* 11, 5 (2007), 596–607.
- [26] Eric Medvet, Alberto Bartoli, Andrea De Lorenzo, and Stefano Seriani. 2020. 2D-VSR-Sim: A simulation tool for the optimization of 2-D voxel-based soft robots. *SoftwareX* 12 (2020), 100573.
- [27] Eric Medvet, Alberto Bartoli, Andrea De Lorenzo, and Stefano Seriani. 2020. Design, validation, and case studies of an optimization-friendly simulator of 2-D Voxel-based soft robots. [arXiv:2001.08617](https://arxiv.org/abs/2001.08617).
- [28] Eric Medvet, Giorgia Nadizar, and Luca Manzoni. 2022. JGEA: a Modular Java Framework for Experimenting with Evolutionary Computation. In *Genetic and Evolutionary Computation Conference Companion*. ACM, New York, NY, USA, 2009–2018.
- [29] Decebal Constantin Mocanu, Elena Mocanu, Peter Stone, Phuong H Nguyen, Madeleine Gibescu, and Antonio Liotta. 2018. Scalable training of artificial neural networks with adaptive sparse connectivity inspired by network science. *Nature communications* 9, 1 (2018), 2383.
- [30] Giorgia Nadizar, Eric Medvet, Stefano Nichele, and Sidney Pontes-Filho. 2023. An experimental comparison of evolved neural network models for controlling simulated modular soft robots. *Applied Soft Computing* 145 (2023), 110610.
- [31] Elias Najarro and Sebastian Risi. 2020. Meta-learning through Hebbian plasticity in random networks. *Advances in Neural Information Processing Systems* 33 (2020), 20719–20731.
- [32] Elias Najarro, Shyam Sudhakaran, and Sebastian Risi. 2023. Towards Self-Assembling Artificial Neural Networks through Neural Developmental Programs. In *Conference on Artificial Life*. MIT Press, Cambridge, MA, USA, 1–10.
- [33] Yael Niv, Daphna Joel, Isaac Meilijson, and Eytan Ruppin. 2001. Evolution of reinforcement learning in uncertain environments: Emergence of risk-aversion and matching. In *European Conference on Artificial Life*. Springer, Berlin, Heidelberg, 252–261.
- [34] Bithika Pal, Arindam Biswas, Sudeshna Kolay, Pabitra Mitra, and Biswajit Basu. 2022. A Study on the Ramanujan Graph Property of Winning Lottery Tickets. In *International Conference on Machine Learning*. PMLR, Baltimore, MD, USA, 17186–17201.
- [35] Fabio Pardo. 2020. Tonic: A Deep Reinforcement Learning Library for Fast Prototyping and Benchmarking. [arXiv:2011.07537](https://arxiv.org/abs/2011.07537).
- [36] Anna R Patten, Suk Yu Yau, Christine J Fontaine, Alicia Meconi, Ryan C Wortman, and Brian R Christie. 2015. The benefits of exercise on structural and functional plasticity in the rodent hippocampus of different disease models. *Brain Plasticity* 1, 1 (2015), 97–127.
- [37] Joachim Winther Pedersen and Sebastian Risi. 2021. Evolving and merging Hebbian learning rules: increasing generalization by decreasing the number of rules. In *Genetic and Evolutionary Computation Conference*. ACM, New York, NY, USA, 892–900.
- [38] Esteban Real, Chen Liang, David R. So, and Quoc V. Le. 2020. AutoML-Zero: Evolving Machine Learning Algorithms From Scratch. [arXiv:2003.03384](https://arxiv.org/abs/2003.03384).
- [39] Christopher Ariel Shaw, Jill C McEachern, and Jill McEachern. 2001. *Toward a theory of neuroplasticity*. Psychology Press, London, UK.
- [40] Andrea Soltoggio, Peter Durr, Claudio Mattiussi, and Dario Floreano. 2007. Evolving neuromodulatory topologies for reinforcement learning-like problems. In *IEEE Congress on Evolutionary Computation*. IEEE, New York, NY, USA, 2471–2478.
- [41] Andrea Soltoggio, Kenneth O Stanley, and Sebastian Risi. 2018. Born to learn: the inspiration, progress, and future of evolved plastic artificial neural networks. *Neural Networks* 108 (2018), 48–67.
- [42] Julian Stier and Michael Granitzer. 2019. Structural analysis of sparse neural networks. *Procedia Computer Science* 159 (2019), 107–116.
- [43] Yushun Tang, Ce Zhang, Heng Xu, Shuoshuo Chen, Jie Cheng, Luziwei Leng, Qinghai Guo, and Zhihai He. 2023. Neuro-Modulated Hebbian Learning for Fully Test-Time Adaptation. In *IEEE/CVF Conference on Computer Vision and Pattern Recognition*. IEEE, New York, NY, USA, 3728–3738.
- [44] E. Todorov, T. Erez, and Y. Tassa. 2012. MuJoCo: A physics engine for model-based control. In *International Conference on Intelligent Robots and Systems*. IEEE/RSJ, New York, NY, USA, 5026–5033.
- [45] Raphael Vallat. 2018. Pingouin: statistics in Python. *The Journal of Open Source Software* 3, 31 (Nov. 2018), 1026.
- [46] R W Williams and K Herrup. 1988. The Control of Neuron Number. *Annual Review of Neuroscience* 11, 1 (1988), 423–453.
- [47] Anil Yaman, Giovanni Iacca, Decebal Constantin Mocanu, Matt Coler, George Fletcher, and Mykola Pechenizkiy. 2021. Evolving plasticity for autonomous learning under changing environmental conditions. *Evolutionary computation* 29, 3 (2021), 391–414.
- [48] Jiaxuan You, Jure Leskovec, Kaiming He, and Saining Xie. 2020. Graph structure of neural networks. In *International Conference on Machine Learning*. PMLR, Online, 10881–10891.
- [49] Karl Zilles. 1992. Neuronal plasticity as an adaptive property of the central nervous system. *Annals of Anatomy-Anatomischer Anzeiger* 174, 5 (1992), 383–391.
- [50] Wendy Zukerman and Andrew Purcell. 2011. Brain’s synaptic pruning continues into your 20s. *New Scientist* 211, 2826 (2011), 9.